Numerical Analysis of Brownian Diffusion-Induced Hybrid Nanofluid Flow Along Thermophoresis

Abubakar Assidiq Hussaini[*], Abdullahi Gamsha Madaki[†], Abubakar Muhammad Kwami[‡], Dauda Gulibur Yakubu[§], Rozaini Roslan[**]

Abstract

In this research work, thermophoresis, Brownian diffusion, thermal radiation, fluid density parameter, magnetic field, and velocity slip effects are examined in relation to the flow and thermal behavior of magnetohydrodynamic (MHD) hybrid nanofluids. Three hybrid nanofluids floating in water (base fluid) are examined: aluminum–silver (Al–Ag), aluminum–copper (Al–Cu), and silver–copper (Ag–Cu). The boundary-layer approximation and Marangoni boundary conditions are used to formulate the governing equations. The governing partial differential equations are then transformed into a coupled system of nonlinear ordinary differential equations using appropriate similarity transformations. This system is subsequently numerically solved using the Runge–Kutta–Fehlberg method in conjunction with the shooting technique. The numerical analysis demonstrates that the temperature distribution within the thermal boundary layer is increased by raising the thermal radiation parameter, thermophoretic effect, and modified fluid density parameter. On the other hand, thermophoresis increases the momentum profile, which encourages fluid motion, while Brownian diffusion has no effect on the momentum field. The outcome of the research also reveals that velocity slip parameter decreases the momentum profile the same effect is observed for temperature profile. Increase in magnetic field intensity raises the momentum profile and decline the temperature profile.

***Keywords*:** Hybrid Nanofluid, Magnetohydrodynamic Flow, Marangoni Convection, Thermophoresis, Brownian Diffusion.

Introduction

A hybrid nanofluid is one novel progression in nanofluid technology. It has emerged as an important development in nanofluid technology because of their ability to deliver superior thermal performance compared with conventional single nanoparticle. They are produced by dispersing two or more dissimilar nanoparticles within a common base

[*]Corresponding Author: Department of Mathematical Sciences, Abubakar Tafawa Balewa University, Bauchi 740272, Nigeria, ahabubakar.pg@atbu.edu.ng

[†]Department of Mathematical Sciences, Abubakar Tafawa Balewa University, Bauchi 740272, Nigeria, agmadaki@atbu.edu.ng

[‡]Department of Mathematical Sciences, Abubakar Tafawa Balewa University, Bauchi 740272, Nigeria, amkwami66@gmail.com

[§]Department of Mathematical Sciences, Abubakar Tafawa Balewa University, Bauchi 740272, Nigeria, dgyakubu@atbu.edu.ng

[**]Department of Mathematics & Statistics, Faculty of Applied Sciences & Technology, University Tun Hussein Onn Malaysia, Pagoh Campus, Muar 84600, Johor, Malaysia, rozaini@uthm.edu.my

fluid, thereby combining the desirable properties of each constituent material. This synergistic interaction enhances the physical, rheological, optical, and thermophysical characteristics of the suspension, resulting in improved heat transfer capability. When compared to mono nanofluids, hybrid nanofluids can lower pressure losses, frictional resistance, and optical extinction while expanding the operating concentration range and improving effective thermal conductivity. They are promising working fluids for next generation thermal management systems because of these benefits. Heat exchangers, heated pipelines, electronic cooling devices, solar energy conversion, refrigeration and air conditioning systems, heating, ventilation, and air conditioning technologies, automotive thermal management, biomedical engineering, aerospace systems, marine technologies, and defense-related engineering applications are all areas in which hybrid nanofluids are being investigated.

Turcu et al. (2006) and Chein & Chuang (2007) groundbreaking paper was a significant turning point in the creation of hybrid nanofluids, which have subsequently gained significant attention in heat-transfer research due to their exceptional thermal properties and wide range of engineering uses. Hybrid nanofluids are very useful for enhancing the thermal performance of Maxwell fluids in sophisticated thermal systems because they combine various nanoparticles within a single base fluid and have enhanced conductive and convective heat-transfer capabilities. In a related study, Hong et al. (2005), Akbar et al. (2024), Nabwey et al., (2024), along with Qureshi et al. (2018) highlighted the importance of hybrid nanofluid flow in improving the functional qualities of materials through nanoscale engineering and identified it as a major catalyst for scientific and technological advancement. The influence of thermophoresis, Brownian diffusion and radiative heat transfer in nanofluid systems has also been investigated extensively in recent years De et al., (2024), Abdul-Basit et al. (2024).

Furthermore, important thermophysical properties, especially thermal conductivity, can be drastically changed by variations in nanoparticle size, volume concentration, and operating temperature. This might have an impact on the fluid's viscosity and general flow characteristics. According to Shah & Ali (2019), hybrid nanofluids perform traditional single particle nanofluids in heat transfer applications because of the synergistic interaction between several nanoparticles. Through advancements at the molecular and cellular levels, nanotechnology has significantly advanced biological science in addition to its function in thermal engineering. For instance, researches by Sridhara et al. (2009), Anwar et al. (2024) along Wong & De Leon (2010) showed how well nanoparticles work in targeted drug delivery, where anticancer

medications can be released in a controlled and site-specific manner with the help of radiation and hyperthermia assisted therapies, increasing treatment precision and reducing side effects.

Each of the three basic mechanisms of heat transfer: conduction, convection, and thermal radiation are essential to thermal management and engineering design. Hussain et al. (2022), Yakubu et at. (2025), Awan et al. (2024), Shah et al. (2024), Wciślik (2020), Wunuji et al. (2023), Shahzad et al. (2024), and Incropera & DeWitt (1990) have all addressed this. While convection transfers heat through fluid motion propelled by either buoyancy factors or externally applied forces, conduction is linked to the transfer of thermal energy through molecular interactions within a substance. Thermal radiation, on the other hand, uses electromagnetic waves to transport energy. Unlike conduction and convection, it doesn't need a material medium, therefore heat can move through clear materials and even through a vacuum.

The impacts of copper-based nanofluids on two- dimensional natural convection heat transport were investigated numerically by Abu-Nada & Oztop (2009). Their findings demonstrated that a discernible improvement in the Nusselt number was obtained even at very low nanoparticle concentrations, indicating a notable improvement in convective heat transfer capacity. Apart from traditional heat transfer systems, hybrid nanofluids have demonstrated efficacy in augmenting thermal transport in porous structures such as metal foams, sandy media, and ceramic matrices. These fluids are now more suitable for a wide range of engineering applications due to their improved thermophysical characteristics. Because effective heat dissipation and energy utilization are crucial in electronic cooling systems, geothermal energy extraction, sophisticated heat exchangers, and high-performance thermal insulation, hybrid nanofluids are becoming more and more popular.

Anwar et al. (2025) investigated MHD hybrid nanofluid flow in the presence of thermal radiation and changing viscosity, but their model did not take into consideration the coupled effects of thermophoretic transport and Brownian diffusion within a Marangoni convection framework. The current study expands their formulation by including these nanoparticle transport methods in addition to improved fluid density and velocity slip effects in order to overcome this constraint. To offer a more thorough knowledge of nanoparticle migration and heat-transfer enhancement in MHD Marangoni flow via porous media, the thermal and flow properties of three hybrid nanofluids viz: Al–Cu, Al–Ag, and Ag–Cu are considered in addition to the effects of thermophoresis along Brownian diffusion. Using tables and graphs to depict the influence of these parameters and other pertinent parameters.

Table 1 presents a succinct summary of the current literature and identifies the research gap that the current study attempts to fill. A more thorough evaluation of heat-transfer enhancement, momentum transport, and nanoparticle migration in MHD Marangoni hybrid nanofluid flow across porous media is made possible by this extension.

Table 1: Identifying the research gap and comparing relevant studies.

Authors	Thermal Rad.	Porous Medium	Brownian Diff.	Thermophoresis	Marangoni Flow	Main Limitation
Abu-Nada & Oztop (2009)	✗	✗	✗	✗	✗	Did not consider hybrid nanofluids or nanoparticle transport mechanisms.
Waini et al. (2019)	✗	✗	✗	✗	✓	Brownian diffusion and thermophoresis effects were neglected.
Olanrewaju et al. (2021)	✓	✗	✗	✗	✗	Marangoni convection and hybrid nanoparticles were not investigated.
Wunuji et al. (2023)	✗	✓	✗	✗	✗	Effects of Brownian motion and thermophoretic transport were not included.
Anwar et al. (2025)	✓	✓	✗	✗	✓	Brownian diffusion and thermophoresis were not considered.
Proposed Study	✓	✓	✓	✓	✓	Addresses the combined effects of Brownian diffusion and thermophoresis on MHD Marangoni hybrid nanofluid flow with thermal radiation, porous medium, modified fluid density, and slip effects.

This is how the rest of the paper is organized. The suggested magnetohydrodynamic hybrid nanofluid model's mathematical formulation, including the governing equations and related boundary conditions, is covered in mathematical analysis. Similarity transformation presents the numerical solution process and the similarity transformations used to reduce the governing equations. The numerical procedure is discussed in Numerical procedure, while, the effects of thermal radiation, thermophoresis, Brownian diffusion, fluid density, magnetic field intensity, and velocity slip on the momentum and temperature fields are thoroughly displayed on graphs and on tables in Numerical results. The results above are discussed in Numerical result Discussion. The work is finally concluded in Conclusion, which summarizes the main conclusions. This research has several areas of applications which are discussed in areas of application, the limitation of this research is also explained under limitations. However, proposed possible avenues for further research is given under future research.

Mathematical analysis

The dispersed nanoparticles are made up of three hybrid combinations: silver–copper (Ag–Cu), aluminum–copper (Al_2O_3–Cu), and aluminum–silver (Al_2O_3–Ag). We considered water as the base fluid. Figure 1 illustrates the physical flow configuration and the corresponding coordinate system considered in the present study.

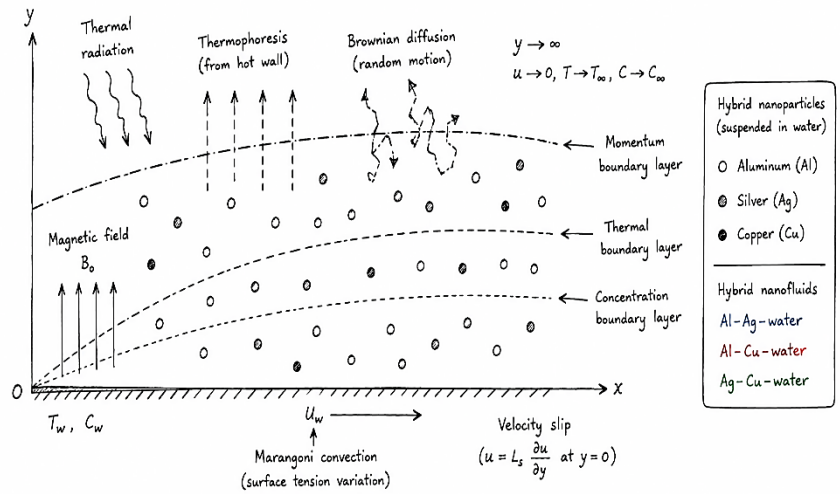

Figure 1: Schematic diagram for the hybrid nanofluid flow.

The hybrid nanofluid's free-stream velocity and Marangoni-driven flow are specified along the x and y-directions, respectively. The stretched sheet's surface temperature is taken to be constant, and the ambient fluid temperature distant from the sheet is represented by T_∞. To examine the magnetohydrodynamic effects on the fluid motion, a uniform magnetic field is provided normal to the flow domain. Furthermore, the surface tension is assumed to vary linearly with temperature in accordance with the Marangoni convection model proposed by Anwar et al. (2025), Waini et al. (2019) and Olanrewaju et al. (2021) is expressed as follows:

$$\gamma = \gamma_0[1 - \overline{\gamma}(T - T_\infty)]$$

In this expression, γ denotes the surface tension at the boundary, while γ_0 represents the rate of change of surface tension with respect to temperature under the assumed linear relationship. Based on these assumptions, the governing flow is described by the following system of partial differential equations, as presented by Anwar et al. (2025):

$$\frac{\partial u}{\partial x} + \frac{\partial v}{\partial y} = 0, \tag{1}$$

$$u\frac{\partial u}{\partial x} + v\frac{\partial u}{\partial y} = \frac{1}{\rho_{hnf}}\frac{\partial u}{\partial y}\left(\mu_{hnf}\frac{\partial u}{\partial y}\right) - \frac{\sigma_{hnf}}{\rho_{hnf}}B_0^2 u - \frac{\mu_{hnf}}{\rho_{hnf}}\frac{u}{k} \tag{2}$$

$$u\frac{\partial T}{\partial x}+v\frac{\partial T}{\partial y}=\frac{k_{hnf}}{(\rho Cp)_{hnf}}\left(\frac{\partial^2 T}{\partial y^2}\right)-\frac{1}{(\rho Cp)_{hnf}}\left(\frac{\partial q_r}{\partial y}\right)+\frac{Q_0}{(\rho Cp)_{hnf}}(T-T_\infty)+\frac{\sigma_{hnf}}{(\rho Cp)_{hnf}}B_0^2u+\frac{\tau\sigma_{hnf}}{(\rho Cp)_{hnf}}\left\{D_B\frac{\partial C}{\partial y}\frac{\partial T}{\partial y}+\frac{D_T}{T_\infty}\left(\frac{\partial T}{\partial y}\right)^2\right\} \quad (3)$$

$$u\frac{\partial C}{\partial x}+v\frac{\partial C}{\partial y}=\frac{D_B k_{hnf}}{(\rho Cp)_{hnf}}\frac{\partial^2 C}{\partial y^2}+\frac{\sigma_{hnf}}{(\rho Cp)_{hnf}}\frac{D_T}{T_\infty}\left(\frac{\partial^2 T}{\partial y^2}\right) \quad (4)$$

supplemented by the following boundary conditions:

$$u=u_s+v_{slip}\left(\frac{\partial u}{\partial y}\right), T=T_\infty+bx^2, -D_B\frac{\partial C}{\partial x}=h_c[C_w-C], y=0, u\to 0, v\to 0, T=T_\infty, C=C_\infty=C_0+d_2x \text{ as } y\to\infty \quad (5)$$

In the present formulation, u and v denote the velocity components in the x and y- directions, respectively. μ_{hnf} denotes the dynamic viscosity of the hybrid nanofluid. Furthermore, k_{hnf}represents its thermal conductivity, σ_{hnf} is the fluid density, and ρ_{hnf} corresponds to the electrical conductivity. Throughout this study, the subscripts f, nf, and hnf refer to the base fluid, nanofluid, and hybrid nanofluid, respectively. In addition, B_0 denotes the applied magnetic field strength, whereas q_r represents the radiative heat flux.

$$q_r=-\frac{4\sigma^*}{3k^*}\frac{\partial T^4}{\partial y}=-\frac{16\sigma^*}{3k^*}T_\infty^3\frac{\partial T}{\partial y}$$

In the radiation model, σ^* *is the Stefan–Boltzmann constant and* k^* denotes the mean absorption coefficient. The permeability of the porous medium is represented by k. While D_B and $D_T$represent the Brownian diffusion coefficient and the thermophoretic diffusion coefficient, respectively. The nanoparticle volume fraction is denoted by C, with C_w and $D_T$indicating the nanoparticle volume fractions at the wall and in the ambient fluid, respectively.

Similarity Transformations

The following similarity transformations are presented in order to make the governing equations easier to solve:

$$\eta=\sqrt{\frac{a}{v}}y, u=\frac{\partial\psi}{\partial y}, v=-\frac{\partial\psi}{\partial x}, \psi=xf(\eta)\sqrt{av}, \theta(\eta)=\frac{T-T_\infty}{T_w-T_\infty}, \phi(\eta)=\frac{C-C_\infty}{C_w-C_\infty} \quad (6)$$

In the present analysis, the dynamic viscosity μ is assumed to vary linearly with temperature and is expressed as:

$$\frac{\mu_\infty}{[1+\gamma(T-T_\infty)]}$$

Upon substituting the similarity transformations of Eq. (6) into the governing equations (1)– (5), the following simplified system of ordinary differential equations is obtained:

$$f'''-\Omega_1\theta'f''+B(1+\Omega\theta)[ff''-(f')^2]-(M+K_1)(1+\Omega\theta)f'=0 \quad (7)$$

$$\left(\frac{1}{Pr}+\frac{4Rd}{3Pr}\right)\theta''+\delta\theta+f\theta'+M\lambda_2(f')^2+Nb\theta'\phi'+Nt(\theta')^2=0 \quad (8)$$

$$\phi''+Scf\phi'+\frac{Nt}{Nb}\theta''=0, \quad (9)$$

The following boundary conditions apply:

$$f'(0)=1+\delta_1 f''(0), \theta(0)=1, \phi(0)=1, \quad (10)$$
$$f'(\infty)=0, \theta(\infty)=0, \phi(\infty)=0,$$

The regulating non-dimensional distance, momentum, temperature, and nanoparticle concentration in the converted formulation are as follows:

$$\eta, f(\eta), \theta(\eta), \phi(\eta)$$
$$\Omega_1=\frac{\Omega}{1+\Omega\theta_1}, \delta_1=\nu_{slip}\sqrt{\frac{a\rho_{hnf}}{\mu_{hnf}}}, Nb=\frac{\tau D_B(C_w-C_\infty)}{\upsilon},$$
$$B=\frac{\rho_{hnf}}{\mu_\infty}, \lambda_2=\frac{\mu_\infty a^2x^2}{(\rho Cp)_{hnf}\upsilon(T_w-T_\infty)}, \Omega=\gamma(T-T_\infty), M=\frac{\sigma_{hnf}B_0^2\upsilon}{a\mu_\infty},$$
$$K_1=\frac{\mu_{hnf}\upsilon}{ak\mu_\infty}, Pr=\frac{\upsilon(\rho Cp)_{hnf}}{k_{hnf}}, Rd=\frac{4\sigma^*T_\infty^3}{k_{hnf}k^*}, \delta=\frac{Q_0}{a(\rho Cp)_{hnf}},$$
$$Nt=\frac{\tau D_T(T_w-T_\infty)}{T_\infty\upsilon},$$

Numerical Procedure

The transformed boundary-value problem was converted into an initial-value problem through the shooting technique. Missing initial conditions were estimated and iteratively adjusted until the far- field boundary conditions were satisfied. Numerical integration was carried out using the fourth- order Runge– Kutta– Fehlberg scheme with convergence tolerance 10^{-6}. Iterations were terminated when successive approximations differed by less than the prescribed tolerance.

Numerical Results

The numerical solutions are obtained using the fourth-order Runge–Kutta–Fehlberg method coupled with the shooting technique are presented in Tables 2–5 and Figures 2–10. The accuracy (validation) and reliability of the present numerical procedure are first established through comparison with previously published results, as summarized in Table 2: the maximum percentage deviation between the present results and published data is less than 0.5%, indicating excellent agreement. Subsequently, the combined effects of the thermophoresis parameter, Brownian diffusion parameter, and thermal radiation parameter on the local Nusselt number and local Sherwood number are presented in Table 3, the qualitative comparison is shown on Table 4, the nomenclature of the parameters as well as abbreviations are on Table 5. Furthermore, the influences of thermal radiation, thermophoresis, Brownian diffusion,

modified fluid density, magnetic field strength, and slip parameter on the momentum and temperature profiles are illustrated in Figures 2– 10.

Table 2: Numerical Result Justification (validation) for $-f''(0)$ ***with published literature for various values of M when B = 1 and Ω = Ω1 = 0.***

Present study	Anwar et al. (2025)	Palani et al. (2019)	Prasad et al. (2012)	Magnetic field parameter
1.000212	1.000012	1.000000	1.000174	0.0
1.224750	1.224749	1.224745	1.224753	0.5
1.414380	1.414239	1.414214	1.414449	1.0
1.581140	1.581138	1.581139	1.581139	1.5
1.732321	1.732115	1.732051	1.732203	2.0

Table 3: Computation of local Nusselt number $(-\theta'(0))$ ***and local Sherwood number*** $(-\phi'(0))$***.***

S/No.	Thermophoresis	Brownian Diffusion	Thermal Radiation	$(-\theta'(0))$	$(-\phi'(0))$
1.	0.1	0.9	0.30	0.8827	0.7248
2.	0.2	0.3	0.40	0.8685	0.7113
3.	0.3	0.5	0.50	0.8534	0.6964
4.	0.4	0.7	0.60	0.8372	0.6802
5.	0.5	0.9	0.70	0.8201	0.6627
6.	0.6	1.3	0.80	0.8023	0.6440
7.	0.7	1.5	0.90	0.7838	0.6243
8.	0.8	1.7	1.00	0.7646	0.6038
9.	0.9	2.0	1.10	0.7448	0.5824
10.	1.0	2.5	1.20	0.7245	0.5603
11.	1.1	2.7	1.30	0.7038	0.5377
12.	1.2	2.9	1.40	0.6826	0.5145
13.	1.3	3.3	1.50	0.6611	0.4910
14.	1.4	3.7	1.60	0.6392	0.4672
15.	1.5	4.0	0.30	0.8827	0.7248

Table 4: Qualitative comparison of the expected thermal performance of the investigated hybrid nanofluids based on thermophysical properties.

Hybrid Nanofluid	Relative Thermal Conductivity	Expected Heat Transfer Capability	Expected Momentum Transport	Overall Thermal Performance
Al–Cu / Water	Moderate	Moderate	Moderate	Good
Al–Ag / Water	High	High	Moderate–High	Very Good
Ag–Cu / Water	Very High	Very High	High	Excellent

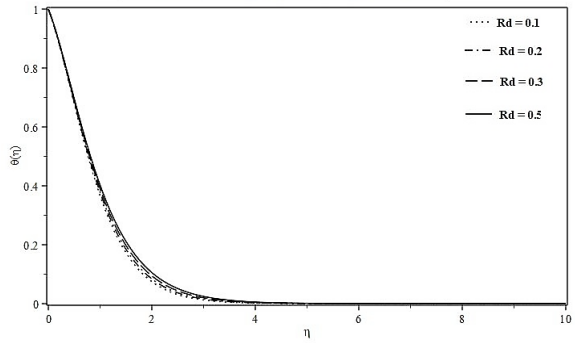

Figure 2: Influence of thermal radiation on the temperature profile.

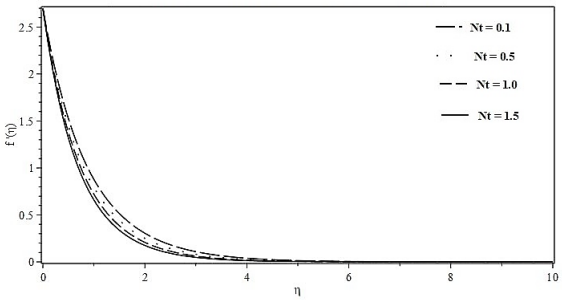

Figure 3: Influence of thermophoresis on the momentum profile.

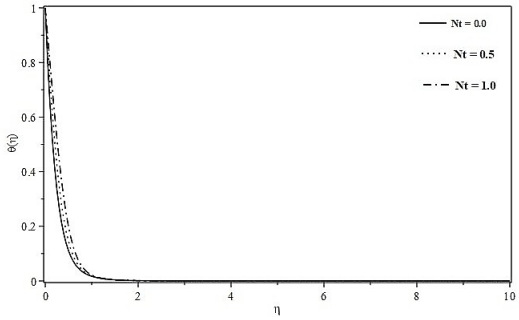

Figure 4: Influence of thermophoresis on the temperature profile.

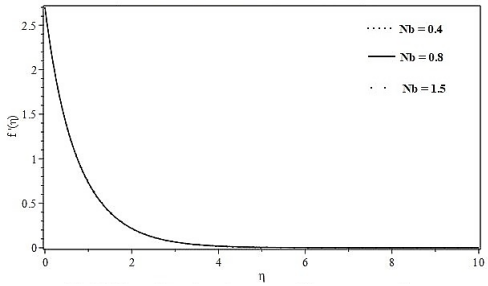

Figure 5: Influence of Brownian diffusion on the momentum profile.

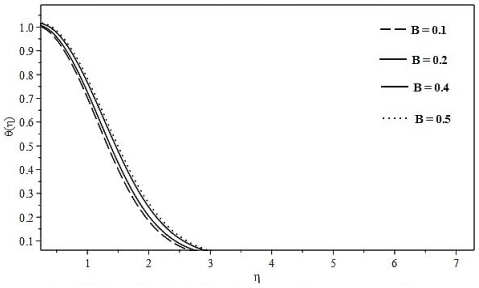

Figure 6: Influence of modified fluid density parameter on the temperature profile.

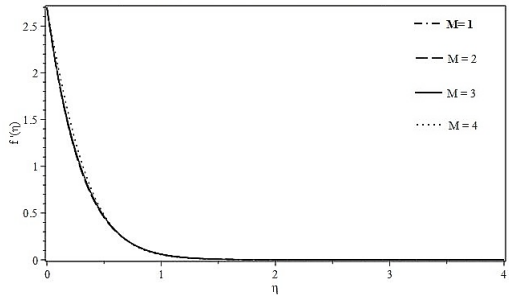

Figure 7: Influence of magnetic parameter on the momentum profile.

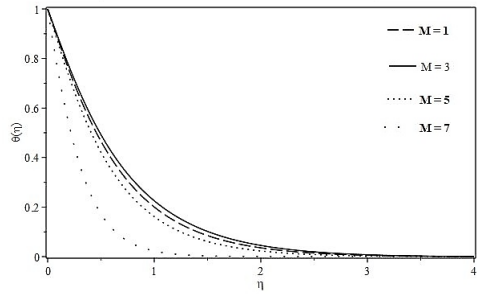

Figure 8: Influence of magnetic parameter on the temperature profile.

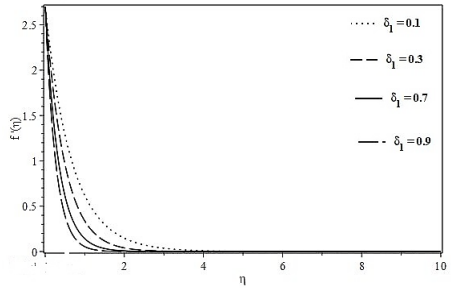

Figure 9: Influence of slip parameter on the momentum profile.

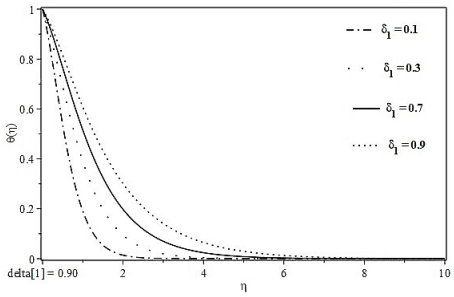

Figure 10: Influence of slip parameter on the temperature profile.

Discussion

The present results are in good agreement with those reported by Anwar et al. (2025), Palani et al. (2019) and Prasad et al. (2012). Similar to their findings, the application of a stronger magnetic field suppresses the velocity profile due to the resistive Lorentz force while enhancing the temperature distribution through the conversion of kinetic energy into thermal energy. Likewise, increasing the thermal radiation parameter increases the fluid temperature by supplying additional thermal energy to the boundary layer. Furthermore, the observed increase in temperature with increasing modified fluid density is also consistent with the trends reported by Anwar et al. (2025). These similarities validate the numerical results obtained in the present study and further confirm the reliability of the proposed mathematical model for analyzing heat transfer characteristics in MHD hybrid nanofluid flow. Additionally, compared with Anwar et al. (2025), the present study extends the analysis by including Brownian diffusion and thermophoretic effects on MHD hybrid nanofluid model, allowing a more comprehensive investigation of nanoparticle transport mechanisms. While Anwar et al. (2025) focused primarily on the effects of variable viscosity, thermal radiation, magnetic field, permeability, and heat source/sink, the present work additionally examines the influence of Brownian motion and thermophoresis on the flow and heat transfer characteristics. Moreover, the inclusion of qualitative comparisons, application prospects, study limitations, and future research directions provides a broader interpretation of the numerical results and enhances the practical relevance of the proposed model. These improvements broaden the scope of the investigation and contribute additional insights into the thermal behaviour of MHD hybrid nanofluids.

Figure 2 illustrates the effect of the thermal radiation parameter on the dimensionless temperature profile of the hybrid nanofluid. The temperature distribution across the thermal boundary layer is found to grow noticeably when the thermal radiation parameter is increased. The strengthening of radiative heat transfer, which enhances conduction by adding more thermal energy to the fluid, is the main cause of the temperature profile's rise. Higher fluid temperatures result from the thermal barrier layer retaining more heat. As a result, the fluid temperature rises and the thermal boundary layer thickens as more heat is retained within the boundary layer stronger thermal radiation allows thermal energy to flow more effectively from the heated surface into the surrounding fluid because it lowers the effective resistance to heat transfer. Consequently, the thermal field spreads farther into the fluid domain and the temperature differential at the wall diminishes. In high-temperature

engineering systems like solar thermal collectors, nuclear reactors, combustion chambers, metallurgical processes, and high-temperature heat exchangers, where radiative effects become considerable, this improvement in thermal energy transport is very crucial. The observed trend is in good agreement with previously published research on magnetohydrodynamic hybrid nanofluids and the accepted theory of radiative heat transfer in boundary-layer flows. after heat radiation has strengthened the thermal field.

Conversely, Figure 3 shows how the thermophoresis parameter affects the dimensionless momentum profile. It is clear that the fluid velocity gradually increases throughout the momentum boundary layer as the thermophoresis parameter is increased. This trend can be explained by the increased migration of nanoparticles under the influence of thermophoretic forces from the heated surface toward areas of lower temperature. However, the influence of thermophoresis parameter over the temperature profile is depicted on Figure 4. For any increase in the values of the parameter there observed a discernible increase in the temperature distribution.

In engineering systems like solar thermal collectors, microchannel heat exchangers, electronic cooling devices, and other high-performance thermal management applications, thermophoresis is crucial for optimizing thermal transport processes. According to earlier research on hybrid nanofluid boundary-layer flows, the observed trend is consistent with the known behavior of thermophoretic transport. Figure 5 illustrates the influence of Brownian diffusion parameter on the dimensionless momentum profile. It is clear that changes in the Brownian diffusion parameter do not significantly alter the velocity distribution across the momentum boundary layer. The impact of the Brownian diffusion parameter on the dimensionless momentum profile is depicted in Figure 5. It is clear that changes in the Brownian diffusion parameter have little to no influence on the fluid velocity because the velocity curves corresponding to various values of this parameter nearly entirely overlap. This behavior results from the fact that, rather than the hydrodynamic behavior of the flow, Brownian diffusion predominantly reflects the random motion of suspended nanoparticles, which primarily affects thermal energy transport and nanoparticle concentration. This is because of this, the forces driving momentum transport are not greatly affected by changes in the Brownian diffusion parameter, and the velocity field generally stays the same. As a result, Brownian diffusion essentially has no effect on the thickness of the momentum boundary layer. These results show that Brownian diffusion very little affects the hydrodynamic properties of the MHD hybrid nanofluid under the current flow

circumstances, however it is anticipated to have a greater impact in the temperature and concentration fields. The impact of the altered fluid density parameter on the dimensionless temperature profile is seen in Figure 6. The findings show that when the adjusted fluid density parameter increases, the temperature inside the thermal boundary layer rises.

Additionally, it be observed in Figure 7, for any increase in the magnetic field intensity parameter there is a corresponding decrease on the momentum profile. Figure 8 depicts the variation in temperature profile when affected by the risen values of magnetic parameter. The temperature is observed to rise with an increase in the parameter values. It can be observed on Figures 9 and 10 respectively; on the influence of velocity slip parameter over momentum and temperature profiles respectively, the momentum profile is seen to rise. This behavior is linked to the decrease in wall shear brought on by fluid slip at the surface, which lessens the fluid's resistance to motion and permits it to flow more freely. As a result, there is less friction, which encourages momentum transit and helps the momentum boundary layer gradually thicken.

Figure 10 shows a different pattern: when the velocity slip parameter rises, the temperature profile falls. Physically, wall slip limits the amount of heat transported into the flow by weakening the thermal connection between the heated surface and the nearby fluid. Lower temperatures and a thinner thermal boundary layer are the results of the fluid absorbing less thermal energy. Heat transmission within the boundary layer is suppressed while fluid motion is enhanced by velocity slip, as seen by the opposite responses of the momentum and temperature fields. These results show that surface slip offers a useful way to control the thermal and hydrodynamic behavior of MHD hybrid nanofluids. In microscale thermal systems, microfluidic devices, coating and extrusion processes, and other technical applications were reducing wall friction while preserving regulated heat transfer is crucial, such control can be especially beneficial.

Conclusion

The impact of thermal radiation, thermophoresis, Brownian diffusion, changed fluid density, magnetic field strength, and velocity slip on the momentum and thermal properties of MHD hybrid nanofluid flow through a porous medium was investigated numerically in this work. The following is a summary of the investigation's main conclusions:

- Thermal radiation increases the temperature distribution
- Increase in the thermophoresis parameter increases both the momentum and temperature fields
- Brownian diffusion has no effect on momentum profile

- A higher modified fluid density elevates temperature distributions
- The application of a stronger magnetic field decreases momentum and increases temperature profile.
- However, velocity slip produces a increase momentum, while decrease temperature profile.

Areas of Applications

This research work has several applications ranging from Industrial Applications: electronic cooling, heat exchangers, solar thermal technologies, power generation systems, microfluidics and MEMS, materials processing and manufacturing, petroleum and geothermal engineering, chemical and process industries. Medical and Biomedical Applications: targeted drug delivery, magnetic hyperthermia, biomedical cooling and thermal therapy, microcirculation and tissue engineering, biomedical diagnostics.

Limitations

The current study is limited to a two-dimensional, constant laminar flow model developed using the boundary-layer approximation. A number of physical effects were excluded from the analysis in order to preserve mathematical tractability and concentrate on the fundamental transport mechanisms. Specifically, temperature-dependent thermal conductivity, turbulence, and nanoparticle aggregation were disregarded. Moreover, no experimental data have been used to verify the computational predictions. Although these presumptions are frequently used in theoretical investigations of hybrid nanofluid flow, they might restrict the current model's direct applicability to more intricate real-world systems. The suggested model's dependability and applicability would be further enhanced by subsequent studies that take these factors into account and contrast the numerical predictions with experimental results.

Future Research Directions

The transport behavior of MHD hybrid nanofluids under the combined effects of thermal radiation, thermophoresis, Brownian diffusion, changed fluid density, and velocity slip is theoretically understood in this work. Even while the suggested model accurately depicts the key elements of the flow and heat-transfer processes, there are still a number of areas that need more research.
In order to depict more realistic engineering systems, future research may expand the current formulation:

- To three-dimensional and unstable flow configurations.

- Additional physical effects such as Joule heating, viscous dissipation, chemical reactions, non-Fourier heat conduction based on the Cattaneo–Christov model, temperature-dependent thermophysical properties, nanoparticle aggregation, and thermal stratification may be included.
- Alternative hybrid and ternary hybrid nanofluids with nanoparticles such graphene, carbon nanotubes, titanium dioxide, and alumina-based composites may also be investigated in future studies

Table 5: Nomenclature.

Physical variables		
Symbol	Description	SI Unit
x, y	Cartesian coordinates	m
u, v	Velocity components	ms^{-1}
Uw	Surface velocity	ms^{-1}
T	Fluid temperature	K
$\boldsymbol{T_w}$	Wall temperature	K
$\boldsymbol{T_\infty}$	Ambient temperature	K
C	Nanoparticle concentration	$kgms^{-3}$
Cw	Wall nanoparticle concentration	$kgms^{-3}$
$\boldsymbol{C_\infty}$	Ambient nanoparticle concentration	$kgms^{-3}$
B_0	Applied magnetic field	T
$\boldsymbol{q_r}$	Radiative heat flux	Wm^{-3}
Q	Heat source/sink coefficient	Wm^{-3}
k	Thermal conductivity	$Wm^{-1}K^{-1}$
k*	Mean absorption coefficient	m^{-1}
K	Permeability	m^2
D_B	Brownian diffusion coefficient	m^2s^{-1}
D_T	Thermophoretic diffusion coefficient	m^2s^{-1}
μ	Dynamic viscosity	Pa s
ν	Kinematic viscosity	m^2s^{-1}
ρ	Density	kgm^{-3}
σ	Electrical conductivity	Sm^{-1}
$(\boldsymbol{\rho Cp})$	Volumetric heat capacity	$Jm^{-3}K^{-1}$
σ*	Stefan-Boltzmann constant	$Wm^{-2}K^{-4}$
ψ	Stream function	m^2s^{-1}
η	Similarity variable	-
f(η)	Dimensionless stream function	-
θ(η)	Dimensionless temperature	-
ϕ(η)	Dimensionless nanoparticle concentration	-
	Dimensionless Parameters	
M	Magnetic parameter	-
$\boldsymbol{\mu_{hnf}}$	Viscosity	-
$(\boldsymbol{\rho Cp})_{\boldsymbol{hnf}}$	capacity	-
T	Temperature,	
$\boldsymbol{T_w}$	Ambient temperature	
$\boldsymbol{T_\infty}$	Wall temperature	
Q	Heat generation/ absorption	
Pr	Prandtl number	-
k	permeability coefficient	-
R	Thermal radiation parameter	-
Nb	Brownian diffusion parameter	-
Nt	Thermophoresis parameter	-
K_1	Permeability parameter	-

B	Modified fluid density parameter	-
Ω	Modified viscosity variation parameter	-
Ω_1	Heat source/sink parameter	-
δ	Variable viscosity parameter	-
δ_1	Velocity slip parameter	-
λ_2	Marangoni parameter	-
	Engineering Quantities	
$f''(0)$	Dimensionless skin-friction coefficient	-
$-\theta'(0)$	Dimensionless local Nusselt number	-
$-\phi'(0)$	Dimensionless local Sherwood number	-
	Subscripts	
f	Base fluid	-
nf	Nanofluid	-
hnf	Hybrid nanofluid	-
w	Wall	-
∞	Ambient	-
	Abbreviations	
RKF45	Runge-Kutta-Fehlberg Method	-
Al_2O_3	Aluminum Oxide	-
Ag	Silver	-
PDE	Partial Differential Equation	-
MHD	Magnetohydrodynamics	-
HNF	Hybrid Nanofluid	-
ODE	Ordinary Differential Equation	-
SWCNT	Single-Walled Carbon Nanotube	-
MWCNT	Multi-Walled Carbon Nanotube	-
EG	Ethylene Glycol	-
Cu	Copper	-

References

Abdul-Basit, M., Imran, M., Madeeha, T., Aboulbaba, E., & Lioua, K. (2024). Numerical analysis of mathematical model for heat and mass transfer through bioconvective Maxwell nanofluid flow subject to Darcy–Forchheimer and Lorentz forces. *International Journal of Heat and Fluid Flow*, 106, 109322.

Abu-Nada, E., & Oztop, H. F. (2009). Effects of inclination angle on natural convection in enclosures filled with Cu-water nanofluid. *International Journal of Heat and Fluid Flow*, 30, 669–678.

Akbar, A. A., Awan, A. U., Nadeem, S., Ahammad, N. A., Raza, N., Oreijah, M., Guedri, K., & Allahyani, S. A. (2024). Heat transfer analysis of Carreau–Yasuda nanofluid flow with variable thermal conductivity and quadratic convection. *Journal of Computational Design and Engineering,* 11(1), 99–109.

De, P., Awan, A. U., & Alzubadi, H. (2025). Mathematical modeling of cross diffusion effect on bioconvective Casson nanofluid over multi slips porous stretching surface. *Numerical Heat Transfer Part B: Fundamentals*, *86*(11), 3781-3800.

De, P., Awan, A. U., & Alzubadi, H. (2025). Mathematical modeling of cross diffusion effect on bioconvective Casson nanofluid over

multi slips porous stretching surface. *Numerical Heat Transfer Part B: Fundamentals*, *86*(11), 3781-3800.

Anwar, M. S. (2025). Heat transfer in MHD convective stagnation point flow over a stretching surface with thermal radiations. *Numerical Heat Transfer, Part A: Applications*, *86*(10), 3130-3145.

Awan, A. U., Shah, S. A. A., Qayyum, S., Alzubadi, H., Ahammad, N. A., & Alroobaea, R. (2024). Mixed convected synchronization of gyrotactic microorganism flow of an Eyring–Powell nanofluid over a riga plate. *ZAMM-Journal of Applied Mathematics and Mechanics/Zeitschrift für Angewandte Mathematik und Mechanik*, *104*(12), e202301055.

Chein, R., & Chuang, J. (2007). Experimental microchannel heat sink performance studies using nanofluids. *International Journal of Thermal Sciences, 46*(1), 57–66.

Hong, T. K., Yang, H. S., & Choi, C. J. (2005). Study of the enhanced thermal conductivity of Fe nanofluids. *Journal of Applied Physics,* 97, 064311.

Hussain, M., Ranjha, Q. A., Anwar, M. S., Jahan, S., & Ali, A. (2022). Eyring–Powell model flow near a convectively heated porous wedge with chemical reaction effects. *Journal of the Taiwan Institute of Chemical Engineers*, 139, 104510.

Bergman, T. L., Lavine, A. S., Incropera, F. P., & DeWitt, D. P. (2011). *Introduction to heat transfer*. John Wiley & Sons.

Nabwey, H. A., El-Hakiem, A. M. A., Khan, W. A., Abdelrahman, Z. M., Rashad, A. M., & Hawsah, M. A. (2024). Magnetic Williamson hybrid nanofluid flow around an inclined stretching cylinder with Joule heating in a porous medium. *Chemical Engineering Journal Advances, 18*, 100604.

Palani, S., Kumar, B. R., & Kameswaran, P. K. (2019). Unsteady MHD flow of a UCM fluid over a stretching surface with higher order chemical reaction. *Ain Shams Engineering Journal, 7*, 399–408.

Prasad, K. V., Sujatha, A., Vajravelu, K., & Pop, I. (2012). MHD flow and heat transfer of a UCM fluid over a stretching surface with variable thermophysical properties. *Meccanica, 47*, 1425–1439.

Qureshi, Z. A., Ali, H. M., & Khushnood, S. (2018). Recent advances on thermal conductivity enhancement of phase change materials for energy storage system: a review. *International Journal of Heat and Mass Transfer*, *127*, 838-856.

Shah, S. A. A., Qayyum, S., Nadeem, S., Alzubadi, H., Ahammad, N. A., Awan, A. U., & Alroobaea, R. (2025). Thermal characterization of Sutterby nanofluid flow under Riga plate: Tiwari and Das model. *Modern Physics Letters B*, *39*(03), 2450421.

Shah, T. R., & Ali, H. M. (2019). Applications of hybrid nanofluids in solar energy, practical limitations and challenges: a critical review. *Solar energy*, *183*, 173-203.

Sridhara, V., Gowrishankar, B. S., Snehalatha, & Satapathy, L. N. (2009). Nanofluids—A new promising fluid for cooling. *Transactions of the Indian Ceramic Society, 68*(1), 1–17.

Turcu, R., Darabont, A., Nan, A., Aldea, N., Macovei, D., Bica, D., Vekas, L., Pana, O., Soran, M. L., Koos, A. A., & Biro, L. P. (2006). New polypyrrole-multiwall carbon nanotubes hybrid materials. *Journal of Optoelectronics and Advanced Materials, 8*(2), 643–647.

Wciślik, S. (2020). Efficient stabilization of mono and hybrid nanofluids. *Energies, 13*(15), 3793.

Wong, K. V., & De Leon, O. (2010). Applications of nanofluids: current and future. *Advances in mechanical engineering*, *2*, 519659.

Wunuji, A. S., Yusuf, A., M., B. S., & Aiyesimi, Y. M. (2023). Magnetohydrodynamics (MHD) stagnation point flow on a stretching sheet with fluid rotation and heat generation. *Asian Journal of Pure and Applied Mathematics, 5*(1), 274–284.

Yakubu, D. G., Abdullahi Isah, & Ali, M. (2025). The dynamic flow of ternary nanofluids with magnetic nanoparticles in an inclined artery exposed to thermal radiation and magnetic fields. *Alexandria Engineering Journal,* 1–10.